

Integration Process Development for Improved Compatibility with Organic Non-Porous Ultralow- k Dielectric Fluorocarbon on Advanced Cu Interconnects

Xun Gu*, Yugo Tomita¹, Takenao Nemoto^{1,2}, Kotaro Miyatani², Akane Saito², Yasuo Kobayashi², Akinobu Teramoto¹, Rihito Kuroda, Shin-Ichiro Kuroki, Kazumasa Kawase³, Toshihisa Nozawa², Takaaki Matsuoka², Shigetoshi Sugawa, and Tadahiro Ohmi^{1,3}

Graduate School of Engineering, Tohoku University, Sendai 980-8579, Japan

¹New Industry Creation Hatchery Center, Tohoku University, Sendai 980-8579, Japan

²Tokyo Electron Technology Development Institute, Inc., Nirasaki, Yamanashi 407-0175, Japan

³Advanced Technology R&D Center, Mitsubishi Electric Corporation, Amagasaki, Hyogo 661-8661, Japan

Received October 14, 2011; accepted January 17, 2012; published online May 21, 2012

Integration of an organic non-porous ultralow- k dielectric, fluorocarbon ($k = 2.2$), into advanced Cu interconnects was demonstrated. The challenges of process-induced damage, such as delamination and variances of both the structure and electrical properties of the fluorocarbon during fabrication, were investigated on Cu/fluorocarbon damascene interconnects. A titanium-based barrier layer, instead of a tantalum-based barrier layer, was used to avoid delamination between Cu and fluorocarbon in Cu/fluorocarbon interconnects. A moisture-hermetic dielectric protective layer was also effective to avoid damage induced by wet chemical cleaning. On the other hand, a post-etching nitrogen plasma treatment to form a stable protective layer on the surface of the fluorocarbon was proposed for the practical minimization of damage introduction to fluorocarbon in the following damascene process, such as post-etching cleaning. © 2012 The Japan Society of Applied Physics

1. Introduction

With the shrinking of feature size of Cu interconnects, more challenges are encountered owing to damage to the low- k dielectrics that appears significantly in efforts to avoid signal propagation delay and to reduce power consumption in ultralarge scale integrated circuits (ULSIs).¹ Etching and wet chemical damage to the porous low- k carbon-doped silicon oxide (SiCO:H) films have been widely studied by many researchers.^{2–6} An alternative organic non-porous fluorocarbon is considered as an indispensable ultralow- k (ULK) dielectric to minimize complexity of LSI fabrication.^{7–11} This new fluorocarbon material was prepared by microwave-excited plasma-enhanced chemical vapor deposition (MWPE-CVD) using an advanced microwave at 2.45 GHz.^{7,8} The microwave plasma indicates a low electron temperature (approximately 1–2 eV) with high plasma density and it sufficiently avoids ion bombardment to the substrate.^{7,8,12–14} Therefore, the fluorocarbon formed by MWPE-CVD showed a much better thermal resistance without film shrinkage at 400 °C than that deposited by the conventional PE-CVD using a parallel plate plasma reactor.^{15,16} The MWPE-CVD fluorocarbon film was, therefore, proposed as a promising ULK film in advanced ULSI devices. This novel non-porous ULK dielectric fluorocarbon formed by MWPE-CVD has been successfully integrated into Cu damascene interconnects in our previous study.^{9–11}

In this study, we explored the integration process-induced damage in delamination and the variances of both structure and electrical characteristics of fluorocarbon induced by wet chemical cleaning and dry etching during Cu/fluorocarbon damascene interconnects fabrication. The integration of the non-porous ULK fluorocarbon without dielectric fluorocarbon degradation into advanced Cu interconnects was also improved.

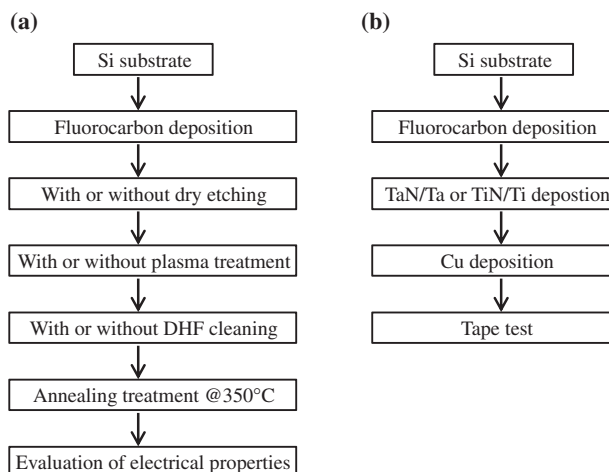


Fig. 1. Process flow of MIS capacitor fabrication.

2. Experimental Procedure

To evaluate the impacts of element processes, such as dielectric protective layer (DPL) and dry etching, on the fluorocarbon film, blanket samples were prepared so as to evaluate the electrical characteristics of fluorocarbon in a metal–insulator–semiconductor (MIS) structure, as shown in Fig. 1(a). An adhesive behavior with different barrier metals between Cu and fluorocarbon was also evaluated using the blanket samples, as shown in Fig. 1(b). In Fig. 1(a), a 150-nm-thick fluorocarbon was formed by MWPE-CVD at a microwave power of 1400 W and a chamber pressure of 3.3 Pa at 350 °C. After dry etching in the fluorocarbon, plasma treatment in nitrogen (N₂) or CF₄ gas was applied. After that, diluted hydrogen fluoride (DHF) was used to remove post-etching residues followed by annealing treatment at 350 °C for 10 min. In Fig. 1(b), tantalum nitride/tantalum (TaN/Ta) or titanium nitride/titanium (TiN/Ti) was formed by physical vapor deposition (PVD) after deposition of the fluorocarbon film. Then, a seed Cu layer

*E-mail address: guxun@ff.niche.tohoku.ac.jp

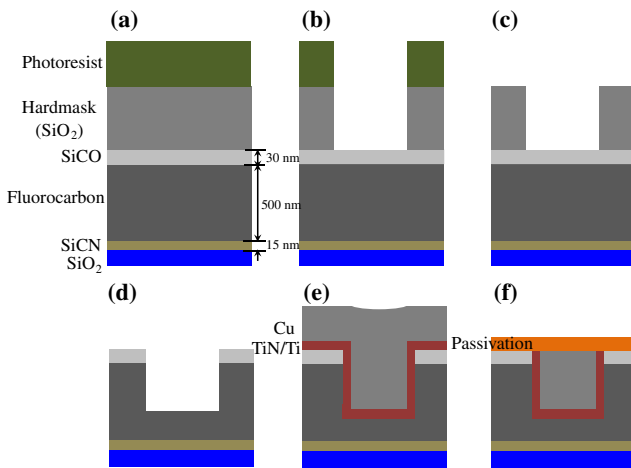


Fig. 2. (Color online) Process flow with cross-sectional images of Cu/fluorocarbon damascene process: (a) deposition, (b) hardmask etching, (c) O₂ ashing, (d) trench etching, (e) metal deposition, and (f) CMP planarization and passivation formation.

was also formed by PVD. After that, an additional annealing treatment at 350 °C for 1 h was applied.

Cu single damascene lines were also prepared for electrical characteristic evaluation. The damascene lines were fabricated in accordance with the process flow illustrated in Fig. 2. A 500-nm-thick fluorocarbon film was formed on a carbon-doped silicon nitride (SiCN) film. The ¹³C chemical structure of the fluorocarbon was measured by nuclear magnetic resonance (NMR) spectroscopy, shown in Fig. 3. A high intensity of the C–F₂ bond and the crosslink structure of C–F and C–C were found in the fluorocarbon formed by MWPE-CVD, compared with that formed using the conventional parallel plate plasma source or polytetrafluoroethylene (PTFE).⁸⁾ Then, a carbon-doped silicon oxide (SiCO) film or a carbon-doped silicon (SiC) film as a DPL was deposited on the fluorocarbon. It was reported that the SiCO film provides a better hermetic barrier against moisture than the SiC film.¹⁷⁾ A photolithography process was run using a KrF stepper. After the etching of trenches in the fluorocarbon dielectric stack layer, plasma treatment in nitrogen (N₂) or CF₄ gas was applied. After that, DHF was used followed by annealing treatment at 350 °C for 10 min. Then, Cu was formed by the electroplate deposition method on a seed Cu layer after TaN/Ta or TiN/Ti formation by PVD. Overburden Cu and TaN/Ta or TiN/Ti were polished by the chemical mechanical planarization (CMP) method.^{18–20)} Citric acid with additives, which has been reported as a suitable solution for cleaning without damage generation in the fluorocarbon film, was used.^{21,22)} A high brush rotation at a low applied down pressure of brush scrubbing cleaning condition, which has been reported to satisfy both good electrical properties and particle removal efficiency, was used for the post-CMP cleaning.^{23–25)} Finally, a passivation SiCN film was formed, then a final annealing treatment was applied at 150 °C.

Leakage current of blanket samples was measured using a mercury prober with a probe area of $1.37 \times 10^{-2} \text{ cm}^2$. A comb pattern of damascene sample with a space of 0.21 μm and a length of 26 cm was also used for line to line leakage current measurements. A line to line capacitance with a

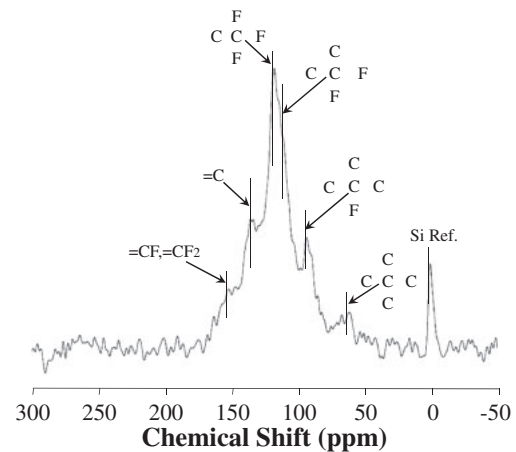


Fig. 3. Chemical structure of the fluorocarbon measured by nuclear magnetic resonance (NMR) spectroscopy.

space of 0.21 μm and a length of 260 cm was also measured using the same pattern with 1 MHz frequency applied voltage. The TriComp 5.0™ simulation tool, which generates field solutions utilizing an automatic conformal mesh generator, was used to explore the electrical field distribution and dielectric constant calculation of damascene lines.

C 1s photoelectron spectra obtained by high-resolution X-ray photoelectron spectroscopy (XPS) using a highly sensitive and high-resolution photoelectron spectrometer equipped with a monochromatic Al Kα radiation source were measured to obtain chemical structures on the surface of the blanket fluorocarbon film to analyze the impacts of dry etching followed by post-etching DHF cleaning at a take-off angle (represents the angle of a photoelectron that escaped) of 90° and a photon energy of 1486.6 eV.^{21,22)} In addition, N 1s photoelectron spectra were also measured by the super photon ring 8 GeV (SPring-8) hard X-ray (7938 eV) photoelectron spectroscopy in the beam line of BL46XU to evaluate the influence of post-etching N₂ plasma treatment (NPT). The hard X-ray spectroscopy system utilizes hard X-ray from high-brilliance synchrotron radiation of SPring-8 to excite high-energy photoelectrons with a large escape depth, achieving a probing depth of approximately 10 nm that is sufficient for the structural analysis of depth inside the material.^{26,27)} The take-off angle (TOA) was set as 80 or 15° to measure either bulk and surface or only the surface of the fluorocarbon film.

3. Results and Discussion

3.1 Selection of barrier metal and DPL

To integrate the organic non-porous ULK dielectric fluorocarbon into Cu damascene interconnects, it is critical to avoid delamination generation during fabrication. Tape tests on the blanket samples, which were followed by the process flow in Fig. 1(b), were carried out on the sample, as shown in Fig. 4. In the area subjected to the tape test, delamination occurred on the whole surface of the sample with TaN/Ta, as shown in Fig. 4(a), although TaN/Ta is widely used as the Cu diffusion barrier and adhesion layers in Cu/porous SiCO(H) interconnects. It was reported that Ta fluoride is generated easily at the interface between Ta and fluorocarbon, which leads to the adhesion problem.^{28,29)}

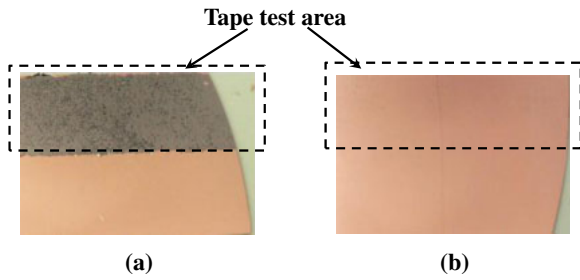


Fig. 4. (Color online) Tape tests on the blanket samples with (a) TaN/Ta and (b) TiN/Ti barrier layers between Cu and fluorocarbon.

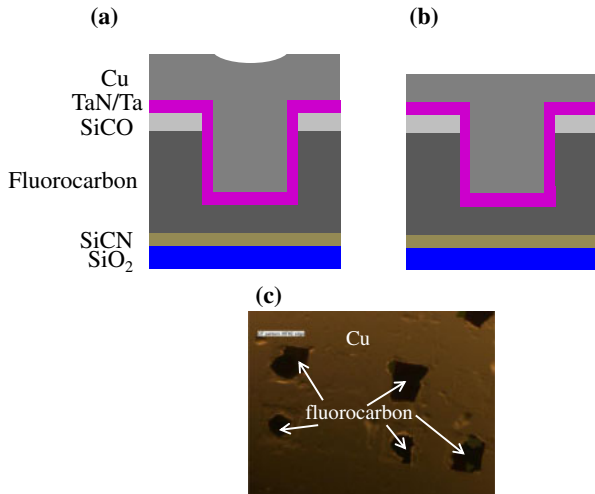


Fig. 5. (Color online) Adhesive behaviors on the damascene sample with TaN/Ta of barrier layer.

On the other hand, the same result was observed in the fabricated damascene sample. TaN/Ta was deposited between the fluorocarbon and Cu layers and then the overburden Cu was polished by CMP after 30 s, as shown in Figs. 5(a) and 5(b). A bird's-eye-view image of this sample was obtained by microscopy, as shown in Fig. 5(c). Delamination was also observed in the interface between fluorocarbon and TaN/Ta. On the other hand, good adhesion was observed after the tape tests on the sample with TiN/Ti, as shown in Fig. 4(b). Therefore, Ti, instead of Ta, was selected as a barrier layer between fluorocarbon and Cu for integration into the damascene process.

The line to line capacitance distribution with a space of 0.21 μm in the Cu-comb pattern with different moisture-hermetic performances of SiCO and SiC films as DPL is shown in Fig. 6. The mean capacitance increased markedly by 20% in the sample with the DPL SiC film, compared with that with the DPL SiCO film. The difference in dielectric constant between blanket SiCO and SiC was found to be less than 5%. This reveals that capacitance of the sample with SiC film shows higher value than that with SiCO film in damascene interconnects. In addition, leakage current on a blanket fluorocarbon with or without DHF cleaning was measured using the mercury prober as the MIS structure, as shown in Fig. 7. No change in the leakage current of dielectric fluorocarbon film was found after DHF cleaning for 2 min. The non-porous structure is considered as the

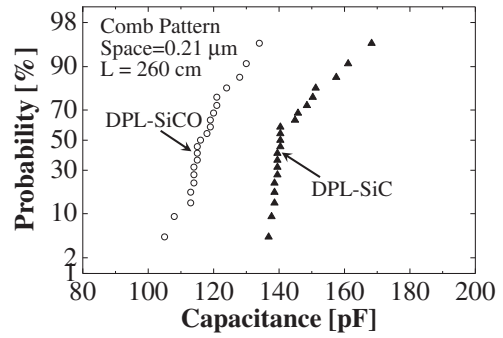


Fig. 6. Line to line capacitance distribution with a space of 0.21 μm in Cu-comb pattern with different moisture-hermetic performances of DPL of SiCO and SiC films.

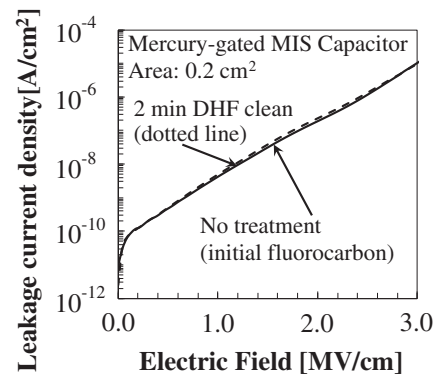


Fig. 7. Leakage current on blanket fluorocarbon samples with different moisture-hermetic performances of DPL of SiCO and SiC films measured using the mercury prober as MIS structures.

reason for the absence of increase in leakage current, which prevents moisture absorption into the bulk fluorocarbon film from chemicals. This shows that the diffusion of moisture from the wet process into the DPL layer, not ULK fluorocarbon, is the possible mechanism and moisture absorption in the bulk DPL SiC film or between the interface of DPL and fluorocarbon increases the line to line capacitance because of the high k -value of water ($k = 81$). Line to line leakage currents with a space of 0.21 μm in the comb pattern are also shown in Fig. 8. The line to line leakage current of the sample with the DPL SiC film is almost one order of magnitude larger than that with the SiCO layer. The absorption of moisture in the bulk DPL SiC film or between the interface of DPL and fluorocarbon promotes Cu ion migration in the interface which is considered as one of the main leakage conduction mechanisms in Cu/low- k interconnects.³⁰⁾

3.2 Application of post-etching plasma treatment

The leakage current densities of the fluorocarbon film at an electric field of 2 MV/cm on blanket fluorocarbon samples with different element processes, which was in accordance with the process flow shown in Fig. 1(a), were measured using the mercury prober as the MIS structures, as shown in Fig. 9. It was found that leakage current density increased with increasing DHF cleaning time when DHF cleaning was carried out after dry etching, while no change was found

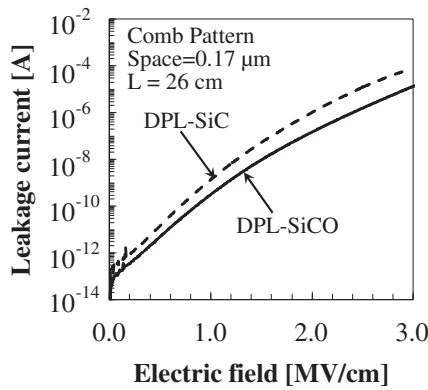


Fig. 8. Line to line leakage currents with different moisture-hermetic performances of DPL of SiCO and SiC films with a space of 0.21 μm in comb pattern.

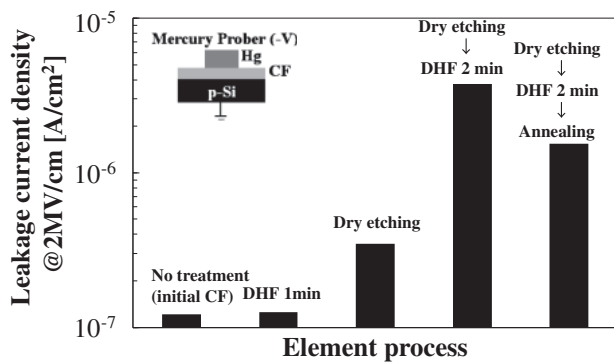


Fig. 9. Leakage current densities of fluorocarbon film at the electrical field of 2MV/cm on a blanket fluorocarbon with different element processes measured using the mercury prober as MIS structure.

after DHF cleaning without dry etching. Only a slight decrease in leakage current was found after the annealing treatment at 350 °C for 10 min. These findings reveal that the leakage current of fluorocarbon was degraded by post-etching DHF cleaning. C 1s photoelectron spectra arising from -C-F₃-, -C-F₂-, -C-F-, and -C-CF_x- were measured by XPS at a photon energy of 1486.6 eV to investigate the variance of structure of the fluorocarbon after dry etching and post-etching DHF cleaning as shown in Fig. 10. The intensity at -C-CF_x- was normalized for comparison with intensities at different peaks. After post-etching DHF cleaning, the intensities at all the -C-F₃-, -C-F₂-, and -C-F- bonds decreased significantly, compared with those after dry-etching only. It was reported that no change in the structure of fluorocarbon was found after chemical dipping only, such as dipping in slurry in CMP, in our previous study.³¹⁻³³ Therefore, this finding reveals that the change in the structure of fluorocarbon during DHF cleaning is a possible mechanism occurring after dry etching and this change in structure probably results in the increase in leakage current during post-etching DHF cleaning. To eliminate the effects of post-etching cleaning on the electrical properties, two kinds of post-etching plasma treatment were investigated. Leakage currents of blanket fluorocarbon in dry etching with post-etching N₂ plasma treatment (NPT) or CF₄ plasma treatment followed by DHF

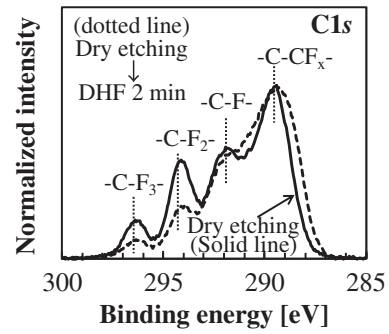


Fig. 10. C 1s photoelectron spectra arising from -C-F₃-, -C-F₂-, -C-F-, and -C-CF_x- analyzed by XPS with a photon energy of 1486.6 eV to investigate the variance of structure after dry etching and post-etching DHF cleaning.

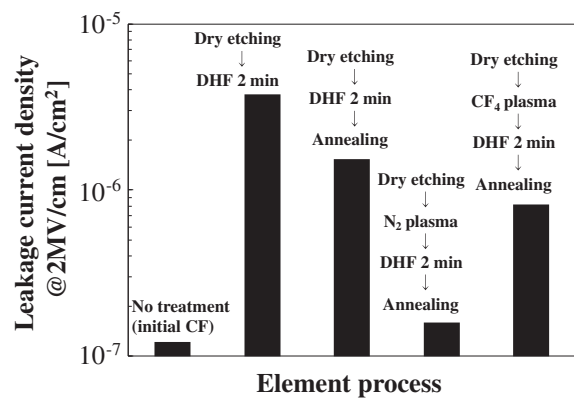


Fig. 11. Leakage current of blanket fluorocarbon in dry etching with post-etching N₂ plasma treatment (NPT) or CF₄ plasma treatment followed by DHF cleaning.

cleaning are shown in Fig. 11. The leakage current of the sample with post-etching NPT decreased to that of initial fluorocarbon, while less improvement of leakage current degradation was also shown in the sample with post-etching CF₄ plasma treatment. On the other hand, these two post-etching plasma treatments were also applied into damascene interconnects. The line to line leakage current distribution in a space of 0.21 μm with or without post-etching NPT or CF₄ plasma treatment is shown in Fig. 12. The sample with post-etching NPT showed a reduced leakage current by one order of magnitude compared with that without post-etching treatment, while no obvious reduction of leakage current was found after post-etching CF₄ plasma treatment. These results are in good agreement with those of the blanket samples, as shown in Fig. 11. This reveals that NPT improves the degradation of line to line leakage current and that NPT is more effective than CF₄ treatment.

To clarify the effect of NPT on the improvement of electrical properties, N 1s spectra measurements of the blanket fluorocarbon film with NPT were conducted by XPS at a photon energy of 7938 eV, as shown in Fig. 13. The intensity of N 1s was generated at TOA 15° (surface only) after NPT of the surface of the fluorocarbon, while no intensity of N 1s was found in the fluorocarbon without post-etching treatment as the initial one. Moreover, a difference in the change in intensity of N 1s at TOA 80° (both surface

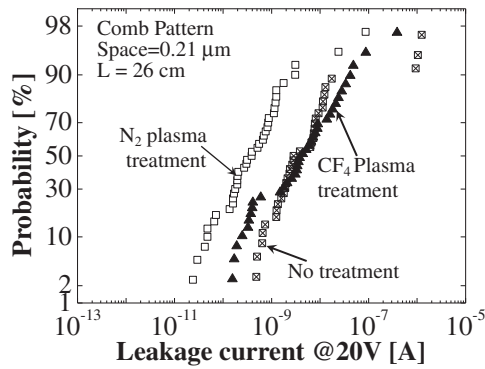


Fig. 12. Line to line leakage current distribution in a space of 0.21 μm with or without post-etching NPT or CF₄ plasma treatment.

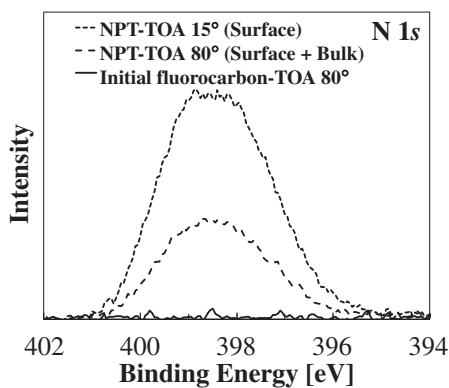


Fig. 13. N 1s spectra measurements of the blanket fluorocarbon film with or without post-etching plasma treatment.

and bulk) and at 15° was found. This reveals that the change in the structure of fluorocarbon is only generated on the surface of the film, and the thickness of the nitrified fluorocarbon layer was reported as less than 5 nm.^{10,11)} In addition, the C 1s photoelectron spectra of the fluorocarbon film were measured by XPS at a photon energy of 1486.6 eV on the samples with or without post-etching DHF cleaning on the etched sample followed by NPT, as shown in Fig. 14. After NPT of the etched sample, no change in the structure of the fluorocarbon was found before and after post-etching DHF cleaning. This shows a big difference from that without NPT, as shown in Fig. 10. These findings reveal that the nitrified fluorocarbon layer was generated on the surface of the fluorocarbon as a stable protective layer that prevents the variance of structural and electrical properties of the fluorocarbon after post-etching cleaning. On the other hand, NPT of the fluorocarbon film was also proved to protect the film from damage induced by CMP.³¹⁻³³⁾ Therefore, NPT is critical and practical for the successful integration of the fluorocarbon film into Cu interconnects without dielectric degradation.

The value of the effective dielectric constant of damascene lines was estimated using the TriComp 5.0 simulator. The electrical field distribution of dielectrics was determined. The effective dielectric constant is calculated as 2.5. The dielectric constants and thicknesses of SiCN, SiCO:H, and SiO₂ were determined from the results of blanket film

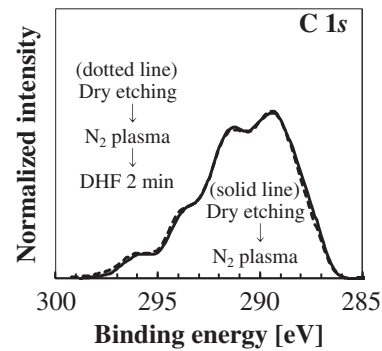


Fig. 14. C 1s photoelectron spectra of the fluorocarbon film analyzed by XPS with a photon energy of 1486.6 eV on the samples with or without post-etching DHF cleaning on the etched sample followed by NPT.

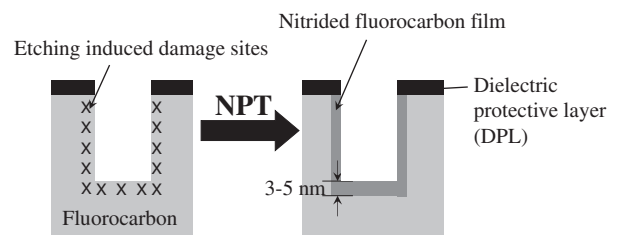


Fig. 15. Model of the two key processes with a moisture-hermetic dielectric protective layer and post-etching N₂ plasma treatment.

measurement and TEM images. Consequently, the dielectric constant of the fluorocarbon layer was calculated as 2.2. This value is the same as that with blanket fluorocarbon film. This result reveals no degradation of the dielectric constant of fluorocarbon following the applications of the DPL SiCO film and NPT method after the fabrication of Cu damascene lines. As a result, the fluorocarbon film showed a remarkable robustness in terms of variation of dielectric constant after fabrication of Cu damascene lines. This film shows better performance than a porous low-*k* film.^{1,2,6)}

A model of the two key processes with a moisture-hermetic dielectric protective layer and post-etching N₂ plasma treatment is illustrated in Fig. 15. A moisture-hermetic dielectric protective layer as well as a stable nitrified fluorocarbon layer is formed as two protective layers on the surface of the dielectric fluorocarbon during fabrication. These two protective layers prevent damage generation induced by wet chemical cleaning and post-etching. Therefore, this organic non-porous ULK fluorocarbon film with these two optimized key processes is considered as an indispensable ULK dielectric for preventing damage generated during Cu damascene fabrication and satisfies the demand for a reduced effective dielectric constant in order to reduce signal propagation delay and power consumption in future ULSI.

4. Conclusions

Damage generated during dry etching and post-etching cleaning that results in the variance of structure and degradation of electrical properties of fluorocarbon has been examined. Post-etching N₂ plasma treatment was applied to form a stable protective layer that against the variance of

structure and damage generated during the post-etching cleaning. A moisture-hermetic dielectric protective layer with a titanium-based barrier layer between fluorocarbon and Cu was also applied to develop the process of integration of ULK fluorocarbon into Cu interconnects with minimized damage. Therefore, a Cu/fluorocarbon damascene integration process without degradation of dielectric fluorocarbon ($k = 2.2$) was successfully developed for future advanced Cu interconnects.

Acknowledgements

The authors express great appreciation to Dr. T. Suwa and Dr. H. Tanaka of Tohoku University for assistance in XPS measurement. The hard X-ray photoelectron spectroscopy experiments were performed at beam line (BL46XU) of Super Photon Ring 8 GeV (SPring-8) with the approval of JASRI as part of the projects of Industrial Application (Project No. 2010A1732).

- 1) M. Ueki, M. Tagami, F. Ito, T. Onodera, I. Kume, N. Furutake, H. Yamamoto, J. Kawahara, N. Inoue, K. Hijioka, T. Takeuchi, S. Saito, N. Okada, and Y. Hayashi: IEDM Tech. Dig., 2008, p. 26.7.
- 2) B. White, A. Knorr, W. Engbrecht, B. Kastenmeier, S. Das, R. McGowan, S. Satyanarayana, and M. Gallagher: *Microelectron. Eng.* **82** (2005) 348.
- 3) B. U. Yoon, S. Kondo, S. Tokitoh, A. Namiki, K. Misawa, K. Inukai, N. Ohashi, and N. Kobayashi: Proc. Int. Interconnect Technology Conf., 2004, p. 13.3.
- 4) T. Yoda, K. Fujita, H. Miyajima, R. Nakata, N. Miyashita, and N. Hayasaka: *Jpn. J. Appl. Phys.* **44** (2005) 3872.
- 5) T. Yoda, Y. Nakasaki, H. Hashimoto, K. Fujita, H. Miyajima, M. Shimada, R. Nakata, N. Kaji, and N. Hayasaka: *Jpn. J. Appl. Phys.* **44** (2005) 75.
- 6) A. Ishikawa, Y. Shishida, T. Yamanishi, N. Hata, T. Nakayama, N. Fujii, H. Tanaka, H. Matsuo, K. Kinoshita, and T. Kikkawa: *J. Electrochem. Soc.* **153** (2006) 692.
- 7) T. Ohmi, M. Hirayama, and A. Teramoto: *J. Phys. D* **39** (2006) 1.
- 8) A. Itoh, A. Inokuchi, S. Yasuda, A. Teramoto, T. Goto, M. Hirayama, and T. Ohmi: *Jpn. J. Appl. Phys.* **47** (2008) 2515.
- 9) X. Gu, T. Nemoto, Y. Tomita, K. Miyatani, A. Saito, Y. Kobayashi, A. Teramoto, S. Kuroki, T. Nozawa, T. Matsuoka, S. Sugawa, and T. Ohmi: *Jpn. J. Appl. Phys.* **50** (2011) 05EB02.
- 10) X. Gu, T. Nemoto, Y. Tomita, A. Shirotori, R. Duyos-Mateo, K. Miyatani, A. Saito, Y. Kobayashi, A. Teramoto, S. Kuroki, T. Nozawa, T. Matsuoka, S. Sugawa, and T. Ohmi: Proc. Int. Interconnects Technology Conf., 2011, p. 1.
- 11) X. Gu, T. Nemoto, Y. Tomita, A. Teramoto, R. Kuroda, S. Kuroki, K. Kawase, S. Sugawa, and T. Ohmi: to be published in IEEE Trans. Electron Devices [DOI: [10.1109/TED.2012.2187659](https://doi.org/10.1109/TED.2012.2187659)].
- 12) H. Tanaka, Z. Chuanjie, Y. Hayakawa, M. Hirayama, A. Teramoto, S. Sugawa, and T. Ohmi: *Jpn. J. Appl. Phys.* **42** (2003) 1911.
- 13) T. Goto, M. Hirayama, H. Yamauchi, M. Moriguchi, S. Sugawa, and T. Ohmi: *Jpn. J. Appl. Phys.* **42** (2003) 1887.
- 14) T. Goto, H. Yamauchi, T. Kato, M. Terasaki, A. Teramoto, M. Hirayama, S. Sugawa, and T. Ohmi: *Jpn. J. Appl. Phys.* **43** (2004) 1784.
- 15) K. Endo and T. Tatsumi: *J. Appl. Phys.* **78** (1995) 1370.
- 16) K. Endo, T. Tatusmi, Y. Matusbara, and T. Horiuchi: *Jpn. J. Appl. Phys.* **37** (1998) 1809.
- 17) US 7,288,205 B2, Oct. 30, 2007.
- 18) X. Gu, T. Nemoto, Y. Sampurno, J. Cheng, S. Theng, A. Philipossian, Y. Zhuang, A. Teramoto, T. Ito, S. Sugawa, and T. Ohmi: *MRS Proc.* **1157** (2009) 1157-E13-03.
- 19) Y. Sampurno, X. Gu, T. Nemoto, Y. Zhuang, A. Teramoto, A. Philipossian, and T. Ohmi: *Jpn. J. Appl. Phys.* **49** (2010) 05FC01.
- 20) X. Gu, T. Nemoto, A. Teramoto, S. Sugawa, and T. Ohmi: Proc. Int. Conf. Planarization/CMP Technology, 2009, p. 22.
- 21) X. Gu, T. Nemoto, A. Teramoto, T. Ito, and T. Ohmi: *J. Electrochem. Soc.* **156** (2009) 409.
- 22) X. Gu, T. Nemoto, A. Teramoto, R. Hasebe, T. Ito, and T. Ohmi: *Solid State Phenom.* **145-146** (2009) 381.
- 23) X. Gu, T. Nemoto, A. Teramoto, T. Ito, S. Sugawa, and T. Ohmi: *ECS Trans.* **19** [7] (2009) 103.
- 24) X. Gu, T. Nemoto, A. Teramoto, M. Sakuragi, S. Sugawa, and T. Ohmi: *J. Electrochem. Soc.* **158** (2011) H1145.
- 25) X. Gu, T. Nemoto, Y. Tomita, A. Teramoto, S. Sugawa, and T. Ohmi: *Jpn. J. Appl. Phys.* **50** (2011) 05EC07.
- 26) T. Aratani, M. Higuchi, S. Sugawa, E. Ikenaga, J. Ushio, H. Nohira, T. Suwa, A. Teramoto, T. Ohmi, and T. Hattori: *J. Appl. Phys.* **104** (2008) 114112.
- 27) T. Suwa, A. Teramoto, Y. Kumagai, K. Abe, X. Li, Y. Nakao, M. Yamamoto, Y. Kato, T. Muro, T. Kinoshita, T. Ohmi, and T. Hattori: *Appl. Phys. Lett.* **96** (2010) 173103.
- 28) S. H. Yang, H. Kim, and J. K. Park: *J. Vac. Sci. Technol. A* **20** (2002) 1769.
- 29) J. P. Chang, H. W. Krautter, W. Zhu, R. L. Opila, and C. S. Pai: *J. Vac. Sci. Technol. A* **17** (1999) 2969.
- 30) J. Noguchi: *IEEE Trans. Electron Devices* **52** (2005) 1743.
- 31) X. Gu, T. Nemoto, Y. Tomita, R. D. Mateo, A. Teramoto, S. Kuroki, S. Sugawa, and T. Ohmi: *ECS Trans.* **34** [1] (2011) 653.
- 32) X. Gu, T. Nemoto, Y. Tomita, A. Teramoto, R. Kuroda, S. Sugawa, and T. Ohmi: *J. Electrochem. Soc.* **159** (2012) H407.
- 33) X. Gu, T. Nemoto, Y. Tomita, R. D. Mateo, A. Teramoto, S. Kuroki, S. Sugawa, and T. Ohmi: Proc. Int. Conf. Planarization/CMP Technology, 2010, p. 51.